Charging Time Characterization for Wireless RF Energy Transfer

Deepak Mishra, Swades De, and Kaushik R. Chowdhury

***Abstract*—Wireless energy transfer to the onboard energy storage element using dedicated radio frequency (RF) energy source has the potential to provide sustained network operations by recharging the sensor nodes on demand. To determine the efficiency of RF energy transfer (RFET), characterization of recharging process is needed. Different from classical capacitor-charging operation, the incident RF waves provide constant power (instead of constant voltage or current) to the storage element, which requires a new theoretical framework for analyzing the charging behavior. This work develops the charging equation for replenishing an energy-depleted storage element by RFET. Since the remaining energy on a sensor node is a random parameter, the RF charging time distribution for a given residual voltage distribution is also derived. The analytical model is validated through hardware experiments and simulations.**

***Index Terms*—Charging time distribution, constant power charging, radio frequency (RF) energy harvesting, wireless energy transfer.**

I. Introduction

In wireless sensor networks (WSNs), field sensors consume energy in sensing, storage, and communication of the sensed data. It is often difficult to access the deployed sensors to replace their batteries. Hence, quite a few recent research works have focused on realizing perennially operating sensor nodes by online replenishment of drained energy. Energy harvesting from the ambient sources such as solar [1], vibration [2], wind [3], ambient radio frequency (RF) [4], and strain from human activities [5] are a few prominent ways to recharge a battery. However, as the availability of sufficient energy from the ambient sources cannot be guaranteed under all circumstances, these sources are unreliable for continuous network operation [6].

Dedicated (on-demand) wireless energy transfer from an RF source is a potential solution to the ambient resource uncertainty [7]. However, the success of RF energy transfer (RFET) relies on accurately predicting the charging efficiency and energy level after a finite charging duration. This is particularly important in the integrated data and energy mule (IDEM) paradigm [8], which extends the concept of the conventional data mule [9]. An IDEM occasionally visits the field nodes and places itself nearby a node for collecting data wirelessly and recharging it via RFET. As the residual energy at a node is a random variable, there is a need to characterize the RF charging time distribution.

In [10], an optimal movement strategy of the mobile charger was proposed that minimizes the overall RF charging delay in the network. In [11], a joint energy-minimum routing and energy-balanced RF charging scheme for rechargeable WSNs was proposed. However, both of these works are based on simplified empirical linear charging model with a constant charging rate assumption. To our best knowledge, no analytical model is available in the literature to characterize RF charging time. Our developed RF charging model in the brief is aimed at filling this gap and providing a robust framework for analyzing the efficacy of the RF harvesting system with mobile chargers to provide sustainable network operation [8].

The problem of estimating the energy level during the charging operation (or the time to fully recharge the onboard storage) of a field sensor is nontrivial. To motivate the problem, we consider the energy storage element as a simple capacitor. To find the efficiency of dedicated RFET, characterization of charging time is required, which is different from the conventional charging of a capacitor from a constant voltage source, e.g., a dc power supply. In charging from a constant voltage source, the initial current is high, and it asymptotically reduces to zero as the capacitor is charged up to the supply voltage. The voltage and current across an initially uncharged capacitor in a series R–C circuit with V_0 as the supply voltage are respectively given as

$$V_C(t) = V_0\left[1 - e^{\frac{-t}{RC}}\right] \qquad I(t) = \frac{V_0}{R} e^{\frac{-t}{RC}}.$$

The main difference between constant voltage charging and RF charging is that, *in the former, the supply voltage is fixed, whereas the latter is a case of constant power charging, where the supply voltage increases and the supply current decreases with the increase in voltage across the capacitor, because the power delivered to the load is constant.* Although the constant voltage charging equations are well known, there are very few analytical formulations on constant power charging. Reference [12] provided the analytical solution for constant power loading of ultracapacitors. It is different from our work in that it is on constant power discharging rather than constant power charging. Reference [13] derived an analytical expression for cell (source) voltage for constant power operation. However, it did not develop the charging time and the capacitor voltage expressions, which are required for charging time characterization. To this end, in this brief, we develop analytical expressions for capacitor voltage, charging time in constant power charging, and charging time distribution as function of the residual voltage.

Manuscript received September 6, 2014; accepted November 18, 2014. This work was supported by the Department of Electronics and Information Technology under Grant 13(2)/2012-CC&BT. This brief was recommended by Associate Editor A. Fayed.

D. Mishra and S. De are with the Department of Electrical Engineering and Bharti School of Telecommunication, Indian Institute of Technology Delhi, New Delhi 110 016, India (e-mail: deepak.mishra@ee.iitd.ac.in; swadesd@ee.iitd.ac.in).

K. R. Chowdhury is with the Department of Electrical and Computer Engineering, Northeastern University, Boston, MA 02115 USA (e-mail: krc@ece.neu.edu).

Color versions of one or more of the figures in this brief are available online at http://ieeexplore.ieee.org.

Digital Object Identifier 10.1109/TCSII.2014.2387732

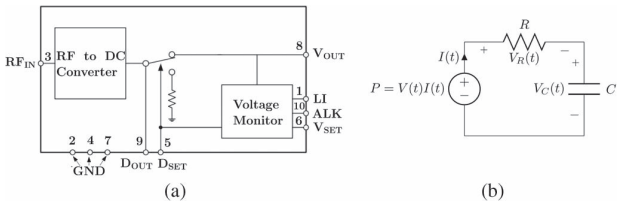

Fig. 1. RF charging module and equivalent circuit model. (a) P1110 functional block [14]. (b) Equivalent $R-C$ circuit.

II. RF Charging Problem

Here, the practical RF charging problem is outlined.

A. RF Charging Characteristics

Charging of a supercapacitor via dedicated RFET is a special case of constant power charging, as the RF power received for recharging the supercapacitor is fixed for an RF source transmitting constant power from a fixed distance. Consider the functional block of P1110 energy harvesting evaluation board in Fig. 1(a) [14] that operates at 915 MHz and harvests the RF input power in the range of -5 to $+20$ dBm. It converts RF energy (radio waves) into dc power, which can be stored in a supercapacitor or used to directly power a circuit. Since the input power is constant, the charging current decreases as the voltage on the $V_{\rm OUT}$ pin increases. P1110 monitors the voltage on the storage element and turns off $V_{\rm OUT}$ when it is fully charged. The maximum output voltage from the harvester IC can be adjusted between 0 and 4.2 V as per requirement. The equivalent series $R-C$ circuit model is shown in Fig. 1(b), where $V(t)$ is the voltage on the $V_{\rm OUT}$ pin, and P is the dc power available after rectification. RF charging time is analytically characterized in Section III, followed by the experimental validation in Section IV.

B. RF Charging Time Distribution

Charging time depends on the residual energy of the node. Thus, the RF charging time can be represented as a function of residual voltage across the supercapacitor before charging, which can be modeled as a random variable. Thus, in a way, RF charging time is also a random variable. RF charging time distribution for two example distributions of residual voltage is derived and validated by simulations in Section V.

III. Analytical Modeling of RF Charging

For deriving the RF charging equations, the dc power available after RF to dc conversion by the P1110 IC is modeled as constant power source with $V_{\rm OUT} = V(t)$ as the source voltage and $I(t)$ as the source current with R as the equivalent series resistance (ESR) of the supercapacitor C [cf., Fig. 1(b)].

A. Constant Power Charging Equation

Applying Kirchhoff's voltage law in the circuit in Fig. 1(b)

$$\begin{aligned} V(t) &= V_R(t) + V_C(t) \\ P &= V(t)\cdot I(t) = [V_R(t) + V_C(t)]\cdot I(t) \\ &= R\cdot\left(\frac{dQ}{dt}\right)^2 + \frac{Q}{C}\cdot\frac{dQ}{dt}. \end{aligned} \tag{1}$$

Note that (1) is a first-order, second-degree, nonlinear, and nonhomogeneous differential equation (DE), with Q as the dependent variable and t as the independent variable. Its explicit solution for Q cannot be obtained. We have solved it for T, i.e., the time required to store Q coulomb of charge in an uncharged capacitor, using the initial condition $Q(t=0)=0$, i.e.,

$$T = \frac{Q^2 + QA + 4C^2RP\ln\left(\frac{A+Q}{\sqrt{4C^2RP}}\right)}{4CP} \tag{2}$$

where $A = \sqrt{Q^2+4C^2RP}$. Call this solution as *method 1*.

As (1) cannot be solved for Q (and thus V_C and I) by solving DE, we take an alternative approach (*method 2*).

Equation (1) is quadratic, with dQ/dt as the unknown. Its solution is

$$\frac{dQ}{dt} = \frac{-\frac{Q}{C} + \sqrt{\left[\left(\frac{Q}{C}\right)^2 + 4RP\right]}}{2R}. \tag{3}$$

To solve for Q, we integrate (3), where, as t goes from 0 to T, an initially uncharged capacitor charges up to Q coulomb, i.e.,

$$\int_0^T \frac{dt}{2R} = \int_0^Q \frac{dQ}{-\frac{Q}{C} + \sqrt{\left[\left(\frac{Q}{C}\right)^2 + 4RP\right]}}. \tag{4}$$

After simplifications, the solution for (4) is obtained as

$$\begin{aligned} \frac{T}{2RC} = \frac{1}{4}\ln\left[\frac{\sqrt{Q^2+4C^2RP}+Q}{\sqrt{Q^2+4C^2RP}-Q}\right] \\ + \frac{\sqrt{Q^2+4C^2RP}}{2\left(\sqrt{Q^2+4C^2RP}-Q\right)} - \frac{1}{2}. \end{aligned} \tag{5}$$

Using $A = \sqrt{Q^2+4C^2RP}$ and $Q = CV_C$ in (5), we get

$$T = \frac{1}{2}RC\left[\frac{2CV_C}{A-CV_C} + \ln\left(\frac{A+CV_C}{A-CV_C}\right)\right]. \tag{6}$$

Expressions (2) and (6) obtained by *methods 1* and *2*, respectively, are equivalent, as demonstrated in Fig. 3(a). In addition, note that T in (2) and (6) is a function of V_C.

Now, the RF charging voltage and current equations as a function of time t are derived. Let

$$Z \triangleq \frac{\sqrt{Q^2+4C^2RP}}{\sqrt{Q^2+4C^2RP}-Q} \tag{7}$$

and replace T by t in (5), to find the voltage and current across an initially uncharged capacitor at any time t. Using (7) and simplifying, (5) can be expressed as

$$(2Z-1)e^{(2Z-1)} = e^{1+\frac{2t}{RC}}. \tag{8}$$

Equation (8) is of the form $ye^y = x$, which can be solved as $y = W(x)$, where $W(x)$ is the Lambert function [15]. For $x > 0$, the solution is denoted as $W_0(x)$ (principal branch). Thus, with the knowledge that $e^{1+(2t/RC)} > 0$, (8) can be solved as

$$Z = \frac{1}{2}\left[1 + W_0\left(e^{1+\frac{2t}{RC}}\right)\right]. \tag{9}$$

From (7), we have the solution for $Q(t)$ as

$$Q(t) = \frac{2C\sqrt{RP}\left(1-\frac{1}{Z}\right)}{\sqrt{1-\left(1-\frac{1}{Z}\right)^2}} \tag{10}$$

where Z is obtained from (9). Note that, in (10), Q has been replaced by $Q(t)$, because it denotes the charge on the capacitor at time t, and thus, it is a function of t.

As $Q = CV_C$, the voltage across the capacitor at time t is

$$V_C(t) = \frac{2\sqrt{RP}\left(1-\frac{1}{Z}\right)}{\sqrt{1-\left(1-\frac{1}{Z}\right)^2}}. \tag{11}$$

From (3), the current across the capacitor at time t is

$$I(t) = \frac{dQ}{dt} = \frac{-\frac{Q(t)}{C} + \sqrt{\left[\left(\frac{Q(t)}{C}\right)^2 + 4RP\right]}}{2R}. \tag{12}$$

B. Charging Time Distribution

RF Charging time T_C is defined as the time required to charge a supercapacitor from a residual value V' to a maximum allowable voltage V_H, which corresponds to the maximum energy that can be stored in the supercapacitor, i.e.,

$$T_C = T(V_H) - T(V') \tag{13}$$

where $T(\cdot)$ is the RF charging time as derived in (6). It may be noted that V' is a random variable, with a lower limit bounded by V_L, which corresponds to the minimum energy required in the supercapacitor for running the sensor node.

We have the cumulative distribution function (CDF) of T_C, i.e.,

$$\begin{aligned} F_{T_C}(t) &= P(T_C \le t) = P\left[T(V_H) - T(V') \le t\right] \\ &= P\left[T(V') > T(V_H) - t\right] \\ &= P\left[V' > \frac{2\sqrt{RP}\left(1-\frac{1}{Z'}\right)}{\sqrt{1-\left(1-\frac{1}{Z'}\right)^2}}\right] \quad \text{(using (11), (6))} \\ &= 1 - F_{V'}(\upsilon) \end{aligned} \tag{14}$$

where υ is the initial residual voltage, i.e.,

$$\upsilon = \frac{2\sqrt{RP}\left(1-\frac{1}{Z'}\right)}{\sqrt{1-\left(1-\frac{1}{Z'}\right)^2}}, \qquad Z' = \frac{1 + W_0\left(e^{1+\frac{2(T(V_H)-t)}{RC}}\right)}{2}. \tag{15}$$

Note that (14) is derived using (11) and (6), because $T(V')$ is the time up to which an initially uncharged capacitor charges to V', and $(2\sqrt{RP}(1-(1/Z'))/\sqrt{1-(1-(1/Z'))^2})$ is the voltage across the capacitor at time $T(V_H) - t$. In addition, (11) is a nondecreasing function of t.

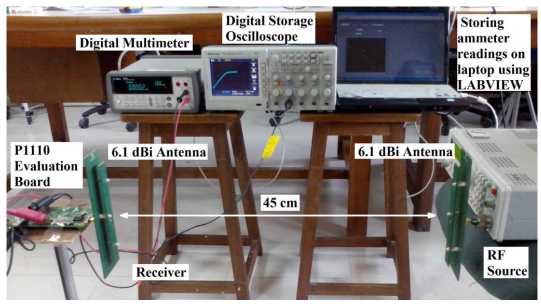

Fig. 2. Experimental setup.

From (14), the probability density function (PDF) of T_C is

$$\begin{aligned} f_{T_C}(t) &= \frac{dF_{T_C}}{dt} = -f_{V'}(\upsilon)\frac{d\upsilon}{dt} \\ &= f_{V'}(\upsilon)\left\{\frac{1}{C}\sqrt{\frac{P}{RZ''}}\right\} \end{aligned} \tag{16}$$

where $f_{V'}(\upsilon)$ is the PDF of the residual voltage, υ is defined in (15), and $Z'' = W_0(e^{1+(2(T(V_H)-t)/RC)})$.

IV. Experimental Validation

We have undertaken systematic experiments to validate the voltage and current across the supercapacitor as derived in (11) and (12), which we describe here.

A. Experimental Setup and Hardware System Parameters

1) RF Source: A HAMEG RF synthesizer HM8135 was used as the RF source that transmits at a power of +13 dBm via 6.1-dBi antenna at 915-MHz frequency.

2) Receiver Node: Receiver node placed at a distance of 0.45 m from RF source consists of a P1110 evaluation board [14] that harvests the input power received from the source via 6.1-dBi antenna and converts it to dc. The evaluation board also consists of a 5.5-V 50-mF supercapacitor to store the converted dc energy.

3) Digital Meters: An Agilent multimeter 34405A was used to record the samples of current through the supercapacitor after every 0.1714 s. These samples were stored in excel file using NI LabVIEW. The voltage across the supercapacitor was measured using a Tektronix TDS 2024B storage oscilloscope. The setup is shown in Fig. 2.

B. System Parameters for Numerical Results

The parameter values for experimental validation and for charging time distribution are as follows. The supercapacitor-related values are the following: capacitance $C = 50$ mF, ESR $R = 0.16\ \Omega$, maximum voltage $V_H = 3$ V, and minimum required voltage $V_L = 2$ V. The RF-source-related values are the following: transmit power $(P_T \cdot G_T) = 19.1$ dBm, receiver antenna gain $G_R = 6.1$ dBi, operating frequency is 915 MHz, charging distance $d = 0.45$ m, path loss exponent in Friis transmission equation (indoor) $\eta = 1.95$, received RF power is 1.3 mW, and harvesting efficiency is 60% [14]. Thus, the harvested dc power $P = 0.8$ mW, the initial charging current [using (12)] $I = 11.21$ mA, and the initial voltage of the

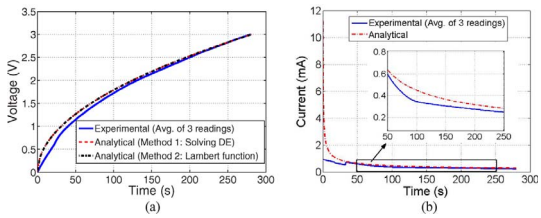

Fig. 3. Experimental validation of RF charging equations. (a) RF charging voltage variation. (b) RF charging current variation.

constant power source $V = 0.0714$ V (using $P = VI$). Hence, the time to charge from V_L to V_H is $T' = 156.25$ s.

C. Experimental Results and Verification of the Analytical Model

Fig. 3(a) and (b) shows closely matched analytical and experimental results. Theoretically, the charging current should be very high at the beginning. However, the instrument has limitations of only recording finite values, and the P1110 has its own surge-protection mechanism to protect the IC from damage. At the start, there is a jump in the current and voltage around the time when the voltage across the supercapacitor reaches 0.7 V. Since the analysis did not account for surge-protection behavior, for verification of correctness of analysis, the starting point of comparative data was taken when the voltage across the supercapacitor crossed 0.8 V. The root-mean-square error (RMSE) of the analytical voltage expression with respect to the mean of three experimental readings is 0.075, and the RMSE of the analytical current expression is 0.063, which are within the allowable upper limit of 0.08 for a model to be considered as a good fit [16]. We consider that these are acceptable as the analytical expressions for the sake of generality do not take into account the consumption by the P1110 IC and assumes that the RF power received is constant.

V. RF Charging Performance Case Studies

We now provide the performance comparison of constant voltage charging and constant power charging based on the theoretical model in Section III-A. This is followed by validation of the charging time distribution derived in Section III-B.

A. Constant Voltage Charging Versus Constant Power Charging

As noted in Section IV-B, the dc power from RF charging is quite low. With the same system parameters as in RF charging, it is difficult to experimentally monitor such low input power of a constant voltage source. Therefore, we resort to simulation-based comparison with constant voltage charging. The circuit parameters [cf., Fig. 1(b)] taken were as follows: source voltage $V_0 = 3$ V, resistance $R = 3\ \Omega$, initial current $I_0 = 1$ A, initial source power $V_0^2/R = 3$ W, and $C = 50$ mF.

The load in the constant power case draws the same power throughout the charging duration, whereas with the constant voltage case, the power drawn decreases with time [cf., Fig. 4(a)]. In other words, the source voltage in constant power charging increases with time [cf., Fig. 4(b)]. As a result, constant power charging is faster. Note that constant power

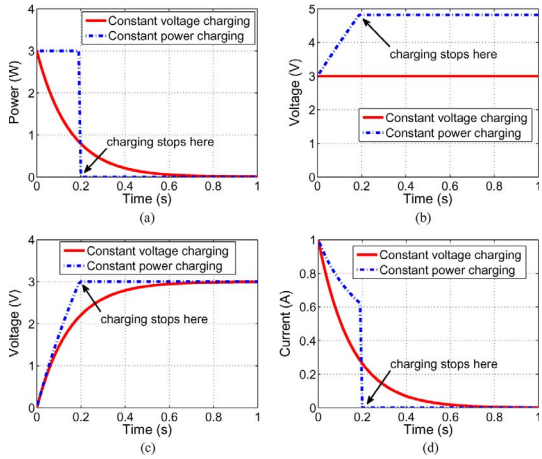

Fig. 4. Constant voltage versus constant power charging. (a) Source power. (b) Source voltage. (c) Capacitor voltage. (d) Current variation.

charging stops when the capacitor gets charged up to $V_H = 3$ V, i.e., at 0.2 s, whereas constant voltage charging takes up to 1 s.

The capacitor's voltage and current are plotted in Fig. 4(c) and (d), respectively. The plots in the constant power case appear to be linear because the input power is very high (3 W) in comparison with the maximum energy to be stored (0.225 J).

B. Validation of RF Charging Time Distribution

The following two cases of voltage distribution are taken.

1) Uniformly Distributed Residual Voltage: Here, V' is uniformly distributed between 2 and 3 V, and its CDF is

$$F_{V'}(x) = \begin{cases} 0 & x \le 2 \\ (x-2) & 2 \le x \le 3 \\ 1 & x \ge 3. \end{cases}$$

Thus, from (14), the CDF of RF charging time is

$$\begin{aligned} F_{T_C}(t) &= 1 - F_{V'}(\upsilon) \\ &= \begin{cases} 0 & t \le 0 \\ (3-\upsilon) & 0 \le t \le T' \\ 1 & t \ge T' \end{cases} \end{aligned} \tag{17}$$

where T' is the time to recharge a supercapacitor from 2 to 3 V ($T' = T(3) - T(2) = 156.25$ s), and υ is the initial residual voltage [cf., (15)]. From (16), the charging time PDF is

$$f_{T_C}(t) = \begin{cases} \frac{1}{C}\sqrt{\frac{P}{RZ''}}, & 0 \le t \le T' \\ 0, & \text{otherwise} \end{cases} \tag{18}$$

because $f_{V'}(x) = \begin{cases} 1, & 2 \le x \le 3 \\ 0, & \text{otherwise.} \end{cases}$

For simulation, 10^6 samples from the preceding uniform distribution were drawn and substituted in place of V' in (13), along with $V_H = 3$ V. The resultant was used to get the simulated CDF and PDF of RF charging time. The analytical CDF and PDF [in (17) and (18), respectively] are plotted against the simulated values in Fig. 5. The mean and variance of RF charging time in this case are 83.40 s and 2040.70 s^2, respectively. Fig. 5(a) shows that, although the simulation result on CDF closely matches with the analysis, it does not

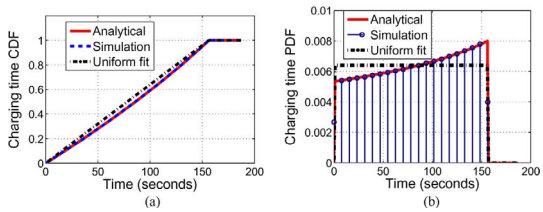

Fig. 5. Uniformly distributed residual voltage case. (a) CDF of RF charging time. (b) PDF of RF charging time.

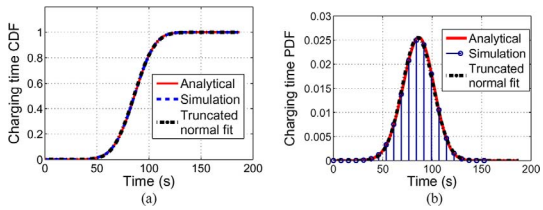

Fig. 6. Truncated normally distributed residual voltage case. (a) CDF of RF charging time. (b) PDF of RF charging time.

exactly match with the corresponding uniform fit in the interval [0, 156.25]. This is also clear from Fig. 5(b), which shows that the shape of the PDF of RF charging time is different from the PDF of uniform distribution, which is a rectangular function.

2) Truncated Normal Distributed Residual Voltage: Here, V' has the truncated normal distribution with a mean $\mu = 2.5$, a variance $\sigma^2 = 0.01$, and $2 \leq V' \leq 3$. The CDF of V' is [17]

$$F_{V'}(x) = \frac{\Phi\left(\frac{x-\mu}{\sigma}\right) - \Phi\left(\frac{2-\mu}{\sigma}\right)}{\Phi\left(\frac{3-\mu}{\sigma}\right) - \Phi\left(\frac{2-\mu}{\sigma}\right)} = \frac{\Phi\left(\frac{x-2.5}{0.1}\right) - 2.87\times10^{-7}}{0.9999994267}$$

where $\Phi(\cdot)$ is the CDF of the standard normal distribution. Hence, from (14)

$$F_{T_C}(t) = \begin{cases} 0, & t \leq 0 \\ 1 - \frac{\Phi\left(\frac{v-2.5}{0.1}\right) - 2.87\times10^{-7}}{0.9999994267}, & 0 \leq t \leq T' \\ 1, & t \geq T'. \end{cases} \quad (19)$$

From (16), the PDF of charging time is

$$f_{T_C}(t) = \begin{cases} \frac{\phi\left(\frac{v-2.5}{0.1}\right)}{0.09999994267} \left(\frac{1}{C}\sqrt{\frac{P}{RZ''}}\right), & 0 \leq t \leq T' \\ 0, & \text{otherwise} \end{cases} \quad (20)$$

where $\phi(\cdot)$ is the PDF of the standard normal distribution.

For simulation, 10^6 samples from the normal distribution with $\mu = 2.5$ and $\sigma^2 = 0.01$ were drawn after neglecting the sample values outside the window [2, 3]. These values were used to substitute V' in (13). The resultant was used to get the simulated CDF and PDF of RF charging time, which are plotted in Fig. 6 against the analytical CDF and PDF in (19) and (20), respectively. The mean and variance of RF charging time in this case are 85.62 s and 244.63 s^2. Fig. 6(a) and (b) shows a close match of the simulation results with the analysis. The CDF of charging time also fits very well with the corresponding truncated normal fit [cf., Fig. 6(a)] lying in the interval [0, 156.25], which is also clear from the fact that charging time follows truncated normal distribution [cf., Fig. 6(b)].

The preceding observations with two chosen residual voltage distributions demonstrate that, although the RF charging time depends on the residual voltage, it does not necessarily follow exactly the same distribution as the underlying residual voltage.

VI. Conclusion

We have shown that RF charging involves practical aspects that go beyond constant power charging and is quite different from conventional constant voltage charging. To this end, RF charging equation and charging time distribution as a function of residual voltage distribution have been developed. The analytical model for RF charging has been experimentally validated. Furthermore, nodal charging time distribution has been derived for uniform and truncated normal distributed residual voltages, which demonstrate that the charging time distribution does not necessarily follow the underlying residual voltage distribution. The analysis and the observations in this brief are useful in evaluating the ability of RF harvesting assisted sustainable network operation.

As a future work, we intend to consider the RF charging profile for the enhanced supercapacitor model that incorporates the nonidealities attributed to substantial leakage currents.

References

[1] V. Raghunathan, A. Kansal, J. Hsu, J. Friedman, and M. B. Srivastava, "Design considerations for solar energy harvesting wireless embedded systems," in *Proc. IEEE ICNP*, Los Angeles, CA, USA, Apr. 2005, pp. 457–462.

[2] S. Roundy, P. K. Wright, and J. Rabaey, "A study of low level vibrations as a power source for wireless sensor nodes," *Comput. Commun.*, vol. 26, no. 11, pp. 1131–1144, Jul. 2003.

[3] M. Weimer, T. Paing, and R. Zane, "Remote area wind energy harvesting for low-power autonomous sensors," in *IEEE PESC/IEEE Power Electron. Spec. Conf.*, Jeju, Korea, Jun. 2006, pp. 1–5.

[4] J. A. Hagerty, F. B. Helmbrecht, W. H. McCalpin, R. Zane, and Z. B. Popovic, "Recycling ambient microwave energy with broad-band rectenna arrays," *IEEE Trans. Microw. Theory Tech.*, vol. 52, no. 3, pp. 1014–1024, Mar. 2004.

[5] J. Gonzalez, A. Rubio, and F. Moll, "Human powered piezoelectric batteries to supply power to wearable electronic devices," *Int. J. Soc. Mater. Eng. Resour.*, vol. 10, no. 1, pp. 34–40, 2002.

[6] Z. A. Eu, W. K. G. Seah, and H.-P. Tan, "A study of MAC schemes for wireless sensor networks powered by ambient energy harvesting," in *Proc. ACM Int. Conf. Wireless Internet*, Maui, HI, USA, Nov. 2008, pp. 1–9.

[7] H. J. Visser, "Indoor wireless RF energy transfer for powering wireless sensors," *Radio Eng.*, vol. 21, no. 4, pp. 963–973, Dec. 2012.

[8] S. De and R. Singhal, "Toward uninterrupted operation of wireless sensor networks," *IEEE Comput. Mag.*, vol. 45, no. 9, pp. 24–30, Sep. 2012.

[9] R. C. Shah, S. Roy, S. Jain, and W. Brunette, "Data mules: Modeling and analysis of a three-tier architecture for sparse sensor networks," *Ad Hoc Netw.*, vol. 1, no. 2, pp. 215–233, Sep. 2003.

[10] L. Fu, P. Cheng, Y. Gu, J. Chen, and T. He, "Minimizing charging delay in wireless rechargeable sensor networks," in *Proc. IEEE INFOCOM*, Turin, Italy, Apr. 2013, pp. 2922–2930.

[11] Z. Li, Y. Peng, W. Zhang, and D. Qiao, "J-RoC: A joint routing and charging scheme to prolong sensor network lifetime," in *Proc. IEEE ICNP*, Vancouver, BC, Canada, Oct. 2011, pp. 373–382.

[12] J. Miller, "Electrical and thermal performance of the carbon–carbon ultracapacitor under constant power conditions," in *Proc. IEEE Veh. Power Propulsion Conf.*, Arlington, TX, USA, Sep. 2007, pp. 559–566.

[13] M. W. Verbrugge and P. Liu, "Analytic solutions and experimental data for cyclic voltammetry and constant-power operation of capacitors consistent with HEV applications," *J. Electrochem. Soc.*, vol. 153, no. 6, pp. A1237–A1245, May 2006.

[14] Powercast P1110 Powerharvester Receiver Datasheet. [Online]. Available: http://www.powercastco.com/PDF/P1110-datasheet.pdf

[15] E. W. Weisstein, "Lambert W-Function," From MathWorld—A Wolfram Web Resource. [Online]. Available: http://mathworld.wolfram.com/LambertW-Function.html

[16] D. Hooper, J. Coughlan, and M. R. Mullen, "Structural equation modeling: Guidelines for determining model fit," *Electron. J. Bus. Res. Methods*, vol. 6, no. 1, pp. 53–60, Apr. 2008.

[17] N. L. Johnson, S. Kotz, and N. Balakrishnan, *Continuous Univariate Distributions*, vol. 1. Hoboken, NJ, USA: Wiley, 1994.